This is the post-print (i.e. final draft post-refereeing) of the publication.
The final publication is available at Elsevier via http://dx.doi.org/10.1016/j.tsf.2015.01.038

Growth and physical properties of highly oriented La-doped (K,Na)NbO_3 ferroelectric thin films

X.Vendrell[1,*], O. Raymond[2], D.A. Ochoa[3], J. E. García[3], L. Mestres[1]

[1]*Departament de Química Inorgànica, Universitat de Barcelona, 08028 Barcelona, Spain.*

[2]*Centro de Nanociencias y Nanotecnología, Universidad Nacional Autónoma de México, AP 14, Ensenada 22860, Baja California, México.*

[3]*Department of Applied Physics, Universitat Politècnica de Catalunya – BarcelonaTech, 08034 Barcelona, Spain.*

Abstract

Lead-free (K,Na)NbO_3 (KNN) and La doped (K,Na)NbO_3 (KNN-La) thin films were grown on $SrTiO_3$ substrates by chemical solution deposition method. The effect of adding different amounts of Na and K excess (0-20 mol%) has been investigated. The results confirm the necessity to add 20 mol% excess amounts of Na and K precursor solutions in order to avoid the formation of the secondary phase, $K_4Nb_6O_{17}$, as is confirmed by X-ray diffraction and Raman spectroscopy. Moreover, when adding a 20 mol% of alkaline metal excess the thin films are highly textured with *out-of-plane* preferential orientation in the [100] direction following the [100] orientation of the substrate. Doping with lanthanum resulted in the decrease in the leakage current density at low electric field, and an increase in the dielectric permittivity across all the temperatures range (80-380 K). Although the (100)-oriented KNN and KNN-La films exhibited rounded hysteresis loops, at low temperature the films showed the typical ferroelectric hysteresis loops.

*Dr. Xavier Vendrell
xavier.vendrell@ub.edu
Telf: +34 934 021 270
Fax: +34 934 907 725

1. Introduction

Excellent piezoelectric and electromechanical properties are obtained in a series of lead-based ferroelectric materials, especially $Pb(Zr,Ti)O_3$ (PZT). Moreover, PZT-based thin films had been widely studied and used for micro-devices over several decades due to the their excellent properties [1,2]. However, environmental issues may ultimately require the replacement of these lead-based materials and thin films in electronic components [3], and the search for lead-free ferroelectrics has recently been intensified. Alkaline niobate-based compounds, especially $(K_{0.5}Na_{0.5})NbO_3$ (KNN), are nowadays being considered as one of the promising lead-free piezoelectric materials because of their good piezoelectricity and a high Curie point [4]. However, serious problems exist for obtaining KNN polycrystalline thin films, because they are usually obtained with high leakage current, and thus with poor ferroelectric properties [5,6]. Moreover, it is important to take special care of the Na/K relationship to obtain high quality thin films [7,8], otherwise low quality ferroelectric properties are obtained. Control of epitaxial growth and stoichiometry are important aspects to take into account when growing high quality thin films. Because of similar crystalline structure of substrates, epitaxial films are technically important for controlling the crystallographic structure, and thus the functional properties of the film.

Many attempts have been made to obtain highly oriented thin films using physical methods, such as radio-frequency magnetron sputtering or pulsed laser deposition [9–11]. Although high quality thin films have been obtained with physical methods, the use of these deposition techniques is not technologically or economically feasible to prepare large areas of thin films. The sol-gel and chemical solution deposition techniques (CSD) are regarded as easier

processes for thin film fabrication. The CSD techniques are very versatile and offer many advantages: low cost, atomic-level homogeneity, mild processing – and therefore compatibility with the silicon technology for semiconductors or ferroelectric memory applications [12] – applicability to multicomponent systems, and easy control of stoichiometry .

The processing of KNN-based thin films by CSD techniques has been addressed in the literature over the last decade but unfortunately only a few of the proposed methods have proven to be reproducible. Although textured films can been obtained using $SrTiO_3$ (STO) substrates [13], the main problems concerning KNN-based thin films are the low stability of the precursor solutions, the low control of stoichiometry and the difficulty in achieving epitaxial films. Furthermore, despite the promising results obtained in bulk lanthanum doped KNN ceramics [14], the introduction of donor dopants into KNN thin films has yet to be explored. Therefore, this work is focused on the synthesis of highly oriented KNN and lanthanum doped KNN thin films by a chemical solution technique using (100)-oriented (STO) single crystal as a substrate. Different excess amounts of Na and K in the solutions are used. The processing steps are detailed and discussed in order to establish a systematic procedure to obtain high quality thin films. The crystallographic and functional properties of the obtained thin films are also investigated.

2. Experimental procedure

The precursor solutions of $(K_{0.5}Na_{0.5})NbO_3$ (KNN) and $[(K_{0.5}Na_{0.5})_{0.985}La_{0.005}]NbO_3$ (KNN-La) were prepared using Na-ethoxide (>95%), K-ethoxide (>95%), La-acetate (>99.9%) and Nb-pentaethoxide (99.95%). Acetylacetone and 2-metoxyethanol were used as the chelating agent and

solvent, respectively. Due to the high reactivity of the alkaline ethoxides to humidity, the precursor solutions of sodium ethoxide, potassium ethoxide and niobium pentaetoxide were prepared in a glove box. To compensate the alkaline metal loss, 0-20 mol% excess amounts of alkaline chemicals were added to the precursor solutions. The alkaline ethoxides and lanthanum acetate solutions together with the chelating agent were mixed and refluxed at 80 ºC for 1 h under N_2. The stoichiometric relationship of the chelating agent was 1:1 with respect to Nb. The niobium pentaethoxide solution was then added and the resultant mixture was refluxed again at 80 ºC for 1 h under N_2. The solution was then distilled to reach a final Nb concentration of 0.3M. The precursor solutions obtained were aged for 24h before being used to deposit thin films.

The KNN and KNN-La precursor solutions were deposited onto STO(100), and SiO_2/Si(100) (Crystec GmbH) substrates by spin-coating in ambient atmosphere at 3000 rpm for 30 s. After each deposition, the precursor films were dried on a hotplate at 150 ºC for 5 min, pyrolyzed at 350 ºC for 5 min and finally annealed at 600 ºC for 3 min. The deposition-drying-pyrolysis-annnealing process was repeated ten times to achieve a total thickness of about 500 nm.

Thermo gravimetric analysis (TGA) and differential thermal analysis (DTA) of the dried gel samples were conducted in air (50 ml/min) using a TGA-sDTA 851e/SF/1100 (Mettler Toledo), from room temperature to 900 ºC with a heating rate of 10 ºC/min. The crystallinity and preferential orientation of the KNN and KNN-La film samples were examined by X-ray diffraction (XRD) using a PANalytical X'Pert PRO MRD diffractometer operated at 45 kV and 40 mA with Cu K_α of 1.54056 Å radiation with a scanning speed of 0.05 º/s and a step of 0.05 º. The Raman scattering spectra of the KNN and KNN-La films deposited

onto SiO_2/Si (100) substrates were obtained on a Jobin-Yvon LabRam HR 800 spectrometer using the 532 nm line of an Ar ion laser. The morphology of film surfaces and film cross-sectional were observed by atomic force microscopy (AFM) (Multimode, Veeco with a Nanoscope IIIa controller) in contact mode using a Si_3N_4 cantilever (Veeco, DNP-S10) and field emission scanning electron microscopy (FE-SEM) (Hitachi 54100), where the voltage conditions were set at 15 kV. The chemical composition of the films was investigated by an electron probe micro analyzer (EPMA) (Cameca SX-50); the wavelength dispersive spectroscopy (WDS) analysis was performed using 15 keV of accelerating voltage and a 20 nA of current. Different reference materials were used for spectra quantification, $SrTiO_3$ for oxygen, albite mineral ($NaAlSi_3O_8$) for sodium, orthoclase mineral ($KAlSi_3O_8$) for potassium and pure niobium for the quantification of niobium. The analysis time for each element and spot was 20 sec/element. The relative errors for each element are shown as a standard deviation calculated from the composition measurement of up to 20 different spots on each thin film. To measure the electric, dielectric and ferroelectric properties, the KNN and KNN-La films were deposited onto 0.7 % niobium doped $SrTiO_3$ substrates (Crystec GmbH), Nb:STO(100), while keeping all the preparation conditions the same as mentioned above. The 100-nm-thick platinum electrodes were deposited on the film surface by DC sputtering. The leakage current and ferroelectric properties were characterized using a standard ferroelectric tester (Precision LC, Radiant Technologies). The relative permittivity and dielectric loss were measured using a Precision LCR Meter (E4980A, Agilent).

3. Results and discussion

3.1. Thermal analysis

TGA-DTA curves were obtained on the dried KNN gel powder in order to determine the pyrolysis and annealing conditions. The stoichiometric KNN gel was dried at 70 ºC for 4 h. A total weight loss of ~ 15 % is shown in TGA-DTA curves (Figure 1). The main weight loss is observed below 550 ºC, which indicates that most of the organics and other volatiles are removed at this temperature. An important weight loss, ~ 5 %, together with an endothermic peak, is observed in TGA curve between 25 - 190 ºC. The weight loss observed at low temperature is related with the H_2O evaporation, but the formation of CO_2 as a result of the decomposition of $NaHCO_3$ and/or $KHCO_3$ should not be excluded as Chowdhury *et al.* have pointed out recently [15]. It should be noted that the global weight loss observed by Chowdhury *et al.*, ~ 21 %, was higher than the global weight loss observed here, ~ 15 %. The main difference between our precursor solutions and those of these authors is that in our case a chelating agent such as acetilacetone was added. The chelating agent could play an important role as a stabilizing agent that prevents reactions with water or CO_2.

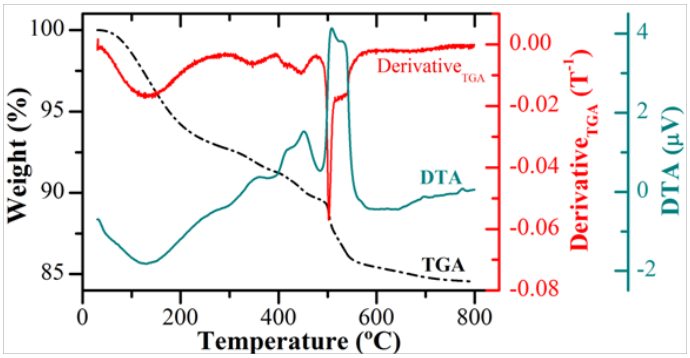

Figure 1. Thermo gravimetric analysis (TGA) and differential thermal analysis (DTA) curves of the dried KNN gel. The derivative curve of TGA analysis is also shown.

At higher temperatures, between 400 – 570 ºC, two exothermic peaks appear due to decomposition reactions of carbonates and a crystallization phenomenon. At temperatures above ~ 600 ºC, the weight loss is lower than 2 %, which could be related to slight loss of sodium and potassium, or a residual loss of CO_2 [16]. Consequently, to obtain homogeneous and high density KNN and KNN-La films, the temperatures of 350 ºC and 600 ºC are chosen as pyrolysis and annealing temperatures, respectively. It should be noted that no differences were observed when analyzing the TGA-DTA curves of the KNN and KNN-La with an excess of alkaline metals.

3.2. Crystalline structure and surface morphology

Figure 2 shows X-ray diffraction (XRD) patterns of KNN and KNN-La thin films, deposited onto STO(100) (Figure 2a, 2b) and SiO_2/Si(100) (Figure 2c, 2d), prepared with precursor solutions using 0 mol%, 10 mol% and 20 mol% of K and Na in excess and keeping the molar ratio Na/K = 1 constant. Thus, 0 mol% corresponds to a 50/50 ratio, 10 mol% to 60/60 and 20 mol% to 70/70. XRD patterns are plotted on a logarithmic scale in order to illustrate better the presence of secondary phases and the growth preferential orientations. The results reveal that the formation of the KNN and KNN-La phase strongly depends on excess amount of Na and K. The formation of the perovskite phase is predominant in all cases. However, due to the high volatility of the alkali metals, the thin films obtained with 0 mol% (50/50) or 10 mol% (60/60) excess of Na and K show the presence of a secondary phase with identified as $K_4Nb_6O_{17}$ (JCPDS #76-0977). Similar behaviour has been observed by different authors [17,18]. Nevertheless, in our study, when the precursor solutions are prepared adding 20 mol% (70/70) excess of alkali metals, the thin films exhibit a

well-crystallized KNN and KNN-La phase and no evidence of secondary phases is detected.

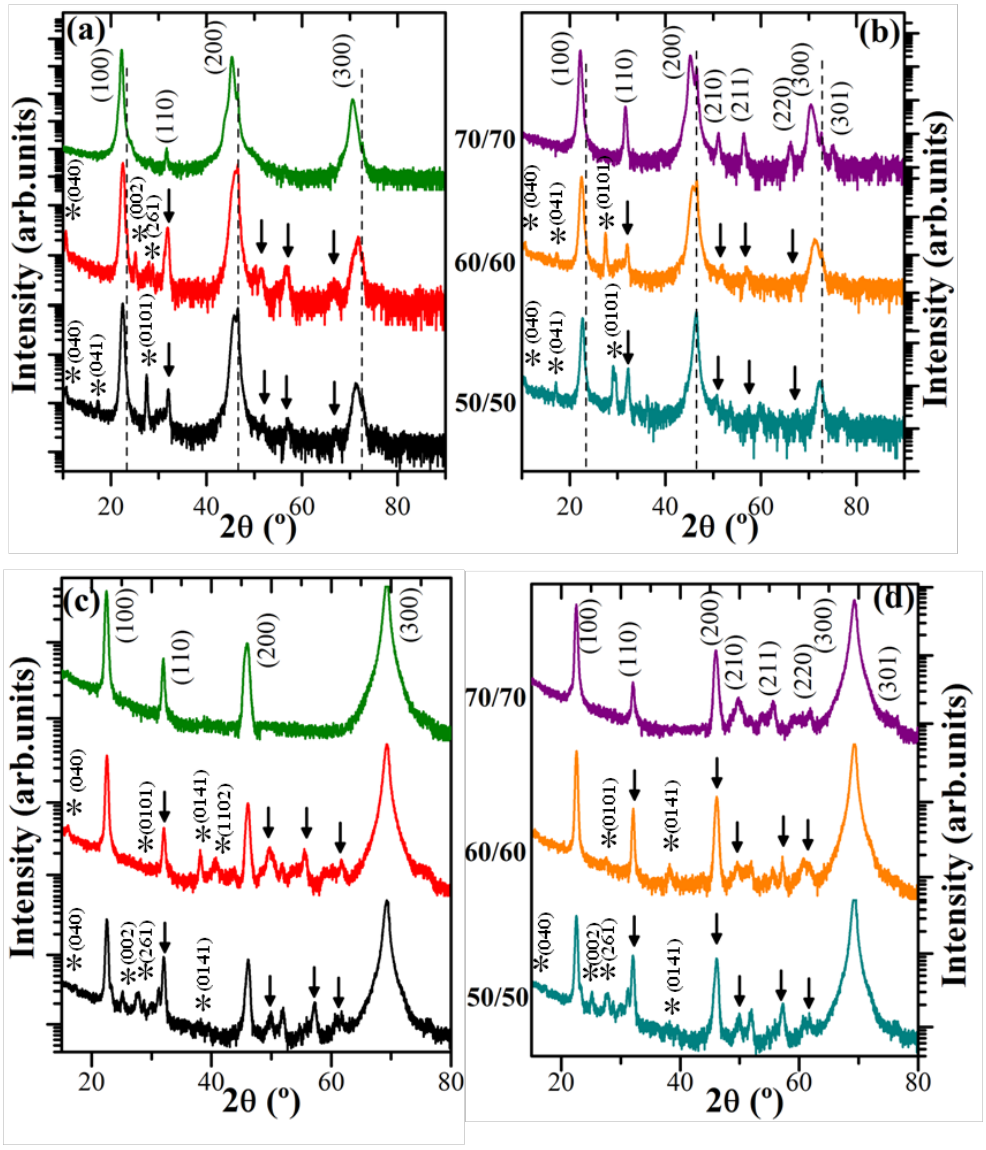

*Figure 2. XRD patterns of KNN (a) and KNN-La (b) thin films deposited on STO(100) substrates and XRD patterns of KNN (c) and KNN-La (d) deposited onto Si(100) substrates, with different excess of Na and K. Substrate peaks are indicated by dashed lines. Arrows show the presence of the some extra peaks associated to the perovskite, but different to the preferred orientation, (100). * indicates the presence of the secondary phase, $K_4Nb_6O_{17}$.*

For simplicity, the orthorhombic symmetry of the KNN compounds can be treated as a pseudo-cubic symmetry due to the close parameters along different

crystallographic orientations of the KNN unit cell [19]. The calculated lattice parameter of KNN(70/70) thin film was estimated to be *a* = 0.399 nm, similar to the values obtained by Tanaka *et al.* [20]. For the thin films doped with La, KNN-La(70/70), the lattice parameter obtained are slightly higher, *a* = 0.404 nm.

Despite the appearance of some signals of various peaks, the XRD patterns of the films show an (100) preferred orientation following the (100) orientation of the STO and SiO_2/Si substrates. As can be observed, the KNN films obtained with low excess amount of alkaline metals, 0 mol% (50/50) and 10 mol% (60/60), show a higher degree of misorientation with the presence of other reflexions different to those of {100} orientation associated to the formation of the secondary phase. It is known that the pyrolysis temperature is a critical processing condition parameter for preferential orientation [13,21]. In our study, all the films were prepared under the same pyrolysis conditions and only the excess amount of Na and K was changed. Thus, as already observed by Kupec *et al.* [22], the stoichiometry could also be a critical parameter affecting the formation of a film with a preferred orientation. Furthermore, the La doped films also show a (100) preferred orientation; however, when adding a 20 mol% excess amount of alkaline metals, the films exhibit some extra peaks (Figure 2b, 2d), which may be associated with the La doping.

Table I. FWHM values of the φ-scan and ω-scan peaks of the STO(100) substrate and KNN thin film prepared with a 20 mol% excess of alkaline metals.

Material	**φ-scan**				**ω-scan**
	Peak 1	Peak 2	Peak 3	Peak 4	
	FWHM (º)				FWHM (º)
STO	0.1804	0.1658	0.1781	0.1761	0.3075
KNN (70/70)	0.8121	0.8079	0.8211	0.8249	0.4728

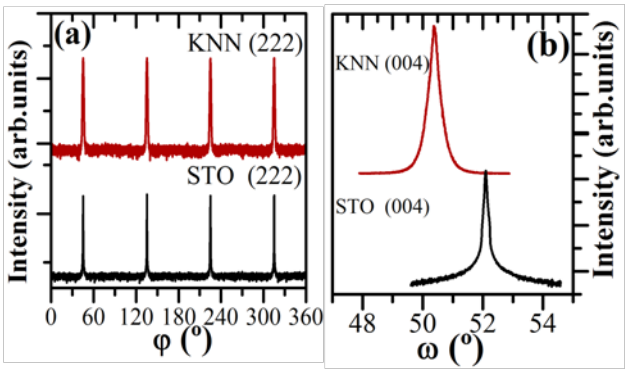

Figure 3. X-ray φ-scan (a) and ω-scan (b) of the pure KNN(70/70) thin films deposited onto STO(100) substrate.

φ-scan and ω-scan were performed to investigate the crystallographic texture degree of the pure KNN(70/70) thin film deposited onto STO(100) substrate. In the X-ray φ-scan the reflection (222), at 2θ = 84.3º, was used; such reflection proved to be appropriate to discern between the film and substrate reflections, which is critical due to the similarity of the lattice parameters. The results, Figure 3a, show four peaks corresponding to the film for every 90º that exactly coincides with the peaks of the substrate, and, as can be observed the film shows a good in-plane ordering. This, in turn, implies that KNN films are coherently *in-plane* oriented. Similar behaviour has been reported when preparing KNN thin films by sol-gel processing using STO(100) as substrate [23]. In addition, the rocking curves or ω-scan, Figure 3b, of the pure KNN(70/70) films deposited onto STO(100) were performed using the (400) reflection, 2θ = 100.8 º. The full width at half maximum (FWHM) of the φ-scan and ω-scan peaks provides important information about the *in-plane* and *out-of-plane* orientation dispersion. Table I shows the FWHM values obtained when analyzing the φ-scan and ω-scan of the STO(100) substrate and the KNN(70/70) film. The film shows higher *in-plane* FWHM values with respect to the substrate ones.

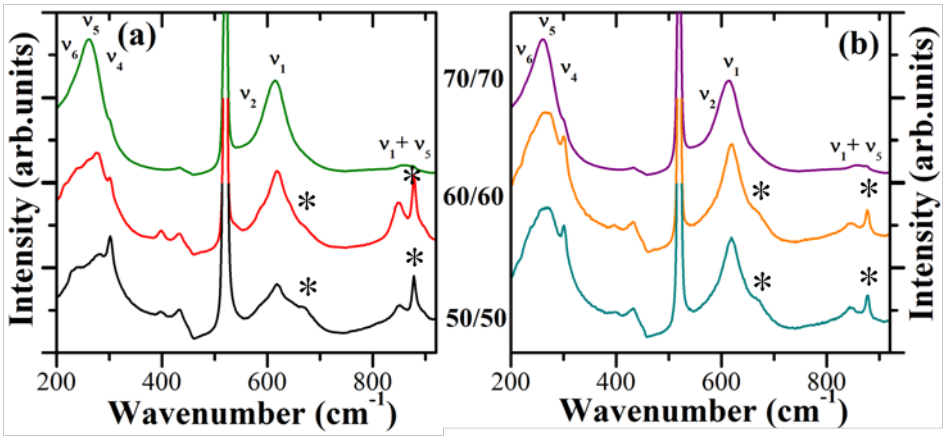

*Figure 4. Raman spectra of the KNN (a) and KNN-La (b) thin films deposited on SiO_2/Si(100) substrates with different excess of Na/K. * indicates the bands corresponding to the secondary phase, $K_4Nb_6O_{17}$.*

As prepared KNN and KNN-La films were analyzed by Raman spectroscopy. The STO substrate shows high intensity Raman active optical modes from 200 to 500 cm^{-1} and from 600 to 800 cm^{-1} (not illustrated here), and the KNN Raman active signals appear at approximately the same Raman displacements [24]. Therefore, due to the high similarities observed between the substrate and the KNN Raman spectra, KNN and KNN-La films were deposited onto SiO_2/Si(100) substrates. Figure 4 shows the Raman spectra of KNN and KNN-La films grown on SiO_2/Si with the different excess amounts of Na^+ and K^+. In all cases a high intensity signal due to the substrate at around 520 cm^{-1} can be observed as well as the typical signals of KNN. Results show the same evolution observed by XRD; at low excess amount of Na^+ and K^+ precursor solutions, the Raman spectra shows the presence of some extra peaks associated to the secondary phase, $K_4Nb_6O_{17}$, at around 670 cm^{-1} and 880 cm^{-1}. Similar behavior has been observed by C.W. Ahn using Pt as substrate [8,25]. Furthermore, when comparing the Raman spectra of the pure and La^{3+} doped KNN films, significant differences can be observed, specifically at low frequency (200 – 350 cm^{-1}). As confirmed by Kakimoto et al. [24], the peaks associated to translation modes of

Na^+/K^+ and K^+ cations versus NbO_6 octahedra appear as weak bands to the left of v_5. Moreover, the vibration modes v_5 and v_6 are more intense and sharper for pure KNN films than the La^{3+} doped ones at low excess amounts of alkali metals, which probably means that there is a lack of alkaline metals at KNN(50/50) and KNN(60/60). Therefore, the different behavior observed between KNN and KNN-La films suggest that La^{3+} is introduced in the A-site of the perovskite. The Raman spectra confirm the obtained results by XRD, i.e. it is necessary to add 20 mol% excess amounts of alkali metal precursor solutions to obtain pure and high quality films.

Table II. Chemical composition, atomic ratio, of KNN and KNN-La thin films with different excess amounts of Na/K, analyzed by EPMA.

Material	Na/K	[K+Na+(La)]/Nb	Na/[K+Na+(La)]
KNN (50/50)	0.89 ±0.06	0.86 ±0.04	0.47 ±0.03
KNN-La (50/50)	0.8 ±0.05	0.92 ±0.03	0.44 ±0.02
KNN (60/60)	0.91 ±0.03	0.99 ±0.01	0.48 ±0.01
KNN-La (60/60)	0.83 ±0.07	0.96 ±0.02	0.45 ±0.02
KNN (70/70)	0.96 ±0.01	1.04 ±0.02	0.49 ±0.01
KNN-La (70/70)	0.96 ±0.04	1.01 ±0.05	0.49 ±0.01
KNN *Nominal*	1	1	0.5
KNN-La *Nominal*	1	0.99	0.497

Table II shows the chemical compositions of the KNN and KNN-La films measured by electron probe micro analyzer (EPMA). The ratio of [(Na+K+(La)]/Nb is lower than 1 when the films are prepared with low excess amounts of alkaline metals (≤ 10 %), indicating high losses of Na^+ and K^+ by volatilization. Moreover, when analyzing the Na/K ratio, lower values than 1 are observed. This effect may be attributed to the easier volatilization of Na^+ than K^+ during the thermal treatment. The higher Na^+ volatilization with respect to K^+ could be related with the formation of the K-rich secondary phase, $K_4Nb_6O_{17}$.

On the other hand, when the films were prepared with a 20 mol% excess of alkaline metals, the [(Na+K+(La)]/Nb and Na/K are close to the stoichiometric composition. Therefore, Na^+ and K^+ volatilization can be compensated for by adding a 20 mol% excess of alkaline metals and high quality thin films can be obtained, as confirmed by XRD and Raman spectroscopy.

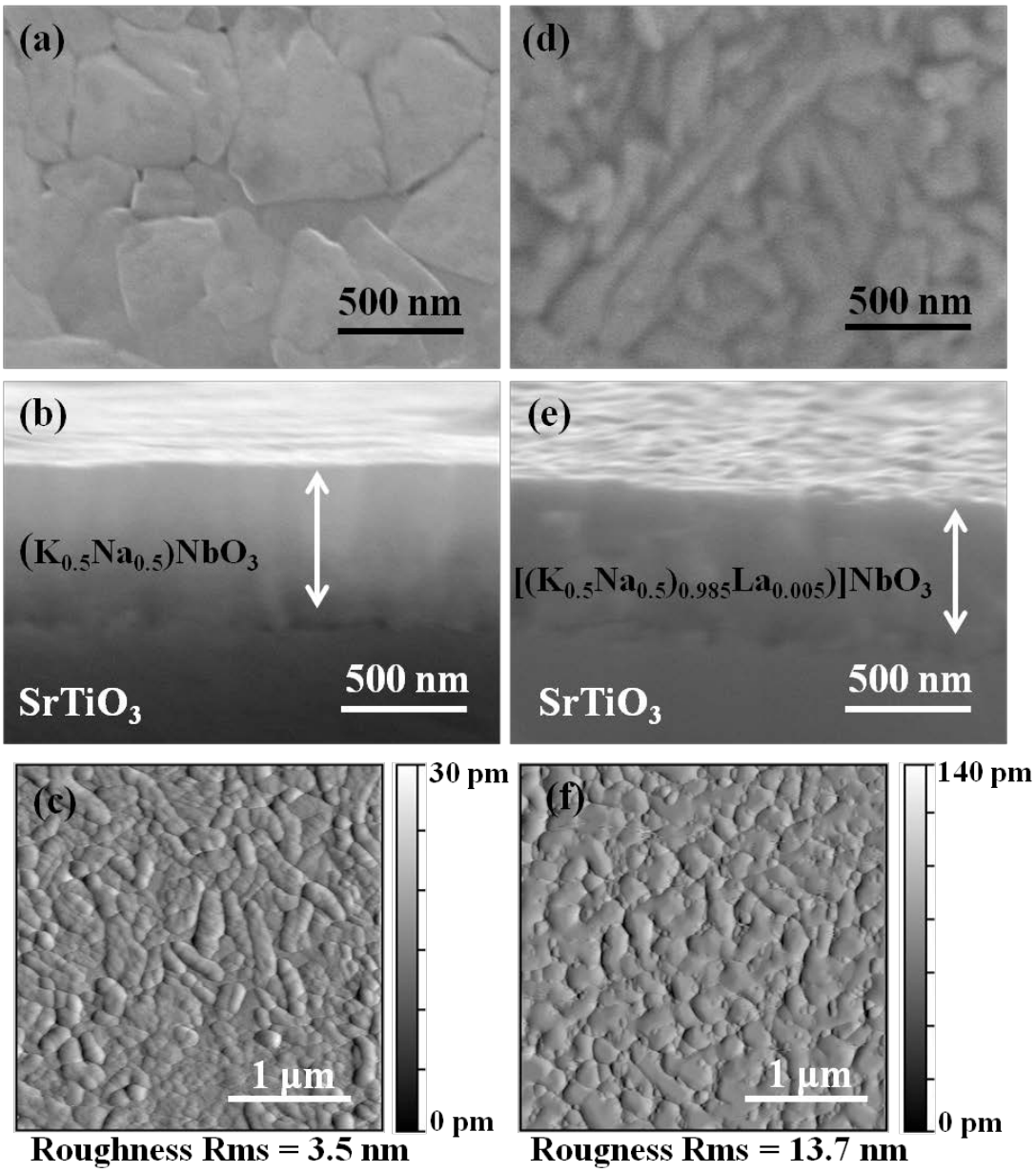

Figure 5. Surface, cross-sectional scanning electron images and AFM images of the KNN (a), (b), (c) and KNN-La (d), (e), (f), thin films, respectively, with a 20 mol% excess of alkaline metals deposited on STO(100) substrates.

Figures 5(a)-(f) show the typical scanning electron microscopy (SEM) surface, SEM cross-section and atomic force microscopy (AFM) surface morphology images of the pure KNN(70/70) and KNN-La(70/70) thin films deposited onto STO substrate. The micrographs of the KNN and KNN-La films show significant differences, as may be seen in Figures 5(a) and 5(d). The pure KNN film presents a triangular-like shapes and a heterogeneous grain size distribution, with grains ranging from ~ 150 to ~ 500 nm. Similar results have been obtained by Kang *et al.* when the annealing temperature is approximately 600 °C [5]. However, the KNN-La film shows rounded and finer grains. The micrographs of the films also reveal a relationship between the (100)-orientation degree and the morphology of the films. For pure KNN with a strong (100)-orientation degree, the film shows a triangular shape and a bigger grain size, while, for the KNN-La film, the grains are rounded without a defined shape. Moreover, the smaller grain size of the KNN-La film is in agreement with the observed when doping with donor dopants such as La^{3+} in ceramics [14]. The cross-section images (Figures 5(b) and 5(e)) reveal that the films are crack-free and dense, with a uniform thickness of approximately 500 nm in both cases. However, whilst the KNN films surface is smooth, the KNN-La films show an increase in surface roughness. The surface morphology evolution observed by AFM, Figures 5(c) and 5(f), is in agreement with that observed by SEM for both 70/70 samples. The root mean square (rms) roughness of the KNN and KNN-La thin films are 3.5 nm and 13.7 nm, respectively. Thus, it is evident that surface morphology as well as surface roughness change when doping with La.

3.3. Electric, dielectric and ferroelectric properties

Figure 6 shows the current density vs. electric field behaviors of KNN(70/70) and KNN-La(70/70) when the electric field is applied from the bottom electrode to the top electrode (positive electric field) at room temperature. For pure KNN the leakage current is relatively low (~10^{-7} A/cm^2) and constant up to an applied field higher than 100 kV/cm, which is similar to that observed by other authors [26]. At this point, the leakage current density rapidly increases (~10^{-4} A/cm^2) when the applied electric field increases. Moreover, for KNN-La films the leakage current density at a low applied electric field is much lower than that observed for pure KNN films (~10^{-9} A/cm^2), and remains practically constant up to an applied field of 70 kV/cm. The leakage current density observed for KNN-La is also lower than the values obtained by some other authors [27]. However, with an increase in the applied electric field, the leakage current density increases drastically and reaches values >10^{-2} A/cm^2 at 150 kV/cm.

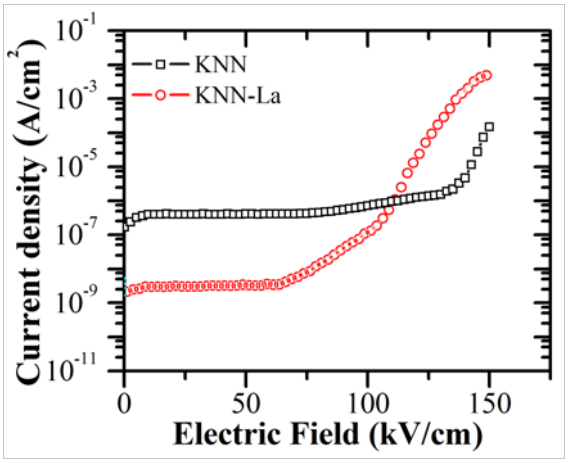

Figure 6. Current density as a function of the applied field for KNN and KNN-La thin films obtained with a 20 mol% excess of alkaline metals.

The increase in the leakage density current when high electric fields are applied may be related with the formation of alkaline ion vacancies (V'_{Na}, V'_{K}) during annealing at high temperatures, as some authors have confirmed [8]. However, as confirmed by EPMA analysis, when adding a 20 mol% excess of alkaline the ratios Na/K and [(Na+K+(La)]/Nb are close to the nominal composition. Therefore, the high leakage density current indicates that other mechanisms are involved. The presence of oxygen vacancies formed during high temperature annealing could be responsible for the increase in the leakage current. However, further investigations of detailed leakage current behavior are needed to clarify the mechanisms for achieving enough efficiency for practical use.

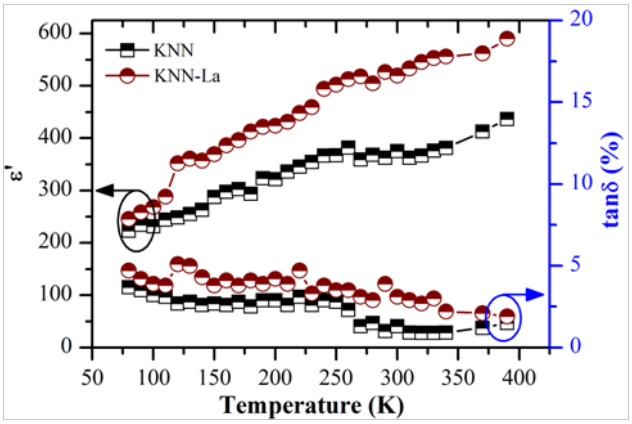

Figure 7. Relative permittivity and loss tangent as a function of temperature for KNN and KNN-La thin films obtained with a 20 mol% excess of alkaline metals.

The dielectric properties of the KNN(70/70) and KNN-La(70/70) films grown on Nb:STO (100) as a function of temperature (80 – 380 K) measured at 1 kHz are shown in Figure 7. Both KNN and KNN-La films show the same behavior, that is, an increase in relative permittivity and a slight decrease of the dielectric loss when the temperature increases. The relative permittivity and dielectric loss values of the KNN and KNN-La obtained are both better than those reported in

by Tanaka et al. [17] and Yan et al. [28]. These results can be explained in terms of higher orientation degree of the pure (100) KNN thin films presented in our work with respect to those obtained by, Tanaka *et al.* and Yan *et al.*. Moreover, the KNN-La thin films show higher relative permittivity values than KNN films. This behavior is in line with the expected results obtained when doping with donor dopants, as already been observed with lanthanum doped KNN ceramics [29]. Therefore, the results confirm that lanthanum is introduced into the KNN lattice.

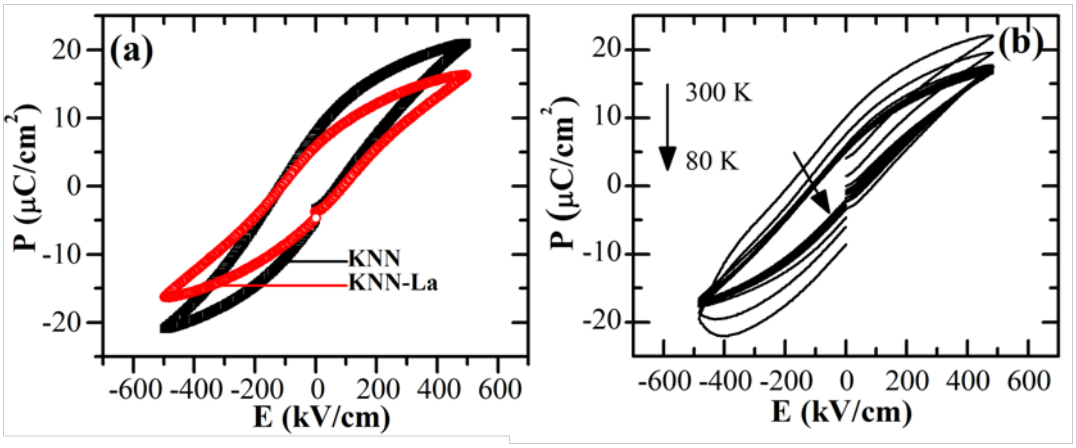

Figure 8. (a) P-E hysteresis loops (measured at 80 K and at 1 kHz) of KNN(70/70) and KNN-La(70/70) thin films; (b) P-E hysteresis loops as a function of temperature of KNN-La(70/70) thin film.

The polarization versus electric field (*P-E)* hysteresis loops (measured at 80 K at 1 kHz) of KNN(70/70) and KNN-La(70/70) grown on Nb:STO (100) are shown in Figure 8(a). The obtained films show a characteristic behavior of a soft ferroelectric material. The remanent polarization of both films only differ slightly, ~8 $\mu C/cm^2$ for KNN and ~6 $\mu C/cm^2$ for KNN-La. Similar values can be found in the literature for KNN systems [13,28]. The remanent polarization values obtained with KNN ceramics are doubled with respect to the thin film ones [30]. This different behavior may be attributable to different effects. Initially, the fact

that KNN possesses an orthorhombic perovskite structure, and so spontaneous polarization occurs along the [110] direction of the cell. For the [100]-oriented films, therefore, the angle between the [110] spontaneous polarization direction and the surface normal of the film is about 45º, and for this reason the observed polarization is lower that observed in KNN ceramics where there is not a defined texture but the volume fraction of crystallites with [110] orientation along the electric field direction is higher. In addition, the different processing of ceramics and thin films may arise in different behaviour due to the presence of defects. Moreover, the grain size effects or the limited thickness effects cannot be discarded. The apparent asymmetry of the hysteresis loops could be attributed to the different bottom-top electrode configuration.

Higher remanent polarization should be expected when doping with lanthanum, as already observed with La^{3+} doped KNN ceramics [14,31]. The different behavior observed between ceramics and thin films could be explained by taking into account the results obtained by Nakashima *et al.*, where the higher values of remanent polarization were obtained for highly oriented films, while the thin films showing lower preferred orientation showed lower values of remanent polarization. Therefore, in our case, the KNN films present a highly (100)-oriented structure, while KNN-La films also show some extra peaks associated to other orientations that are different to that preferred. Consequently, the KNN-La film does not show higher remanent values as should be expected when doping.

The ferroelectric properties of KNN-La films with an increase in temperature are shown in Figure 8(b). When approaching to room temperature the hysteresis loops show a rounded shape, which indicates that the film contains some

leakage components. Higher fields could not be applied due to the high increase in the leakage current density, as is observed in Figure 6. The same behavior was observed with KNN thin films leaky like ferroelectric loops are obtained when reaching room temperature.

4. Summary

Highly (100)-oriented (K,Na)NbO_3 and $[(K_{0.5}Na_{0.5})_{0.985}La_{0.005}]NbO_3$ thin films were prepared through a chemical solution deposition method on $SrTiO_3$ substrates. The φ-scan and ω-scan have confirmed that the KNN thin films were grown with a cube-on-cube fashion on the $SrTiO_3$ substrates. The necessity to adding a 20 mol% excess of alkaline metal precursor solutions to compensate for the Na^+ and K^+ volatilization during the annealing treatment has been established; otherwise, the secondary phase $K_4Nb_6O_{17}$ is obtained, as confirmed by XRD and Raman spectroscopy. When doping with lanthanum, the thin films show a lower leakage current density at low electric fields which should be helpful for the development of low leakage current films. KNN-La films exhibit higher relative permittivity values as expected when a perovskite ferroelectric is doped with donor dopants. While the films exhibited rounded hysteresis loops at room temperature, indicating that they contain some leakage components. Further optimization of the synthesis conditions, particularly by controlling the formation of oxygen vacancies, is necessary to improve the electric properties of the films.

Acknowledgements

The authors would like to thank the Spanish Government MAT2013-48009-C4-2-P Project, the Catalan Government PIGC project 2009-SGR-0674, and the DGAPA-UNAM IN113312 and Conacyt 127633 projects, for their financial

support. The authors are grateful to M.Sc. P. Prieto and to the Scientific and Technological Centers of the University of Barcelona for their technical support.

References

[1] P. Murralt, Ferroelectric thin films for micro-sensors and actuators : a, J. Micromechanics Microengineering. 10 (2000) 136–146.

[2] N. Setter, D. Damjanovic, L. Eng, G. Fox, S. Gevorgian, S. Hong, A. Kingon, H. Kohlstedt, N. Y., Park, G. B. Stephenson, I. Stolitchnov, A. K. Taganstev, D. V. Taylor, T. Yamada, S. Streiffer, Ferroelectric thin films: Review of materials, properties, and applications, J. Appl. Phys. 100 (2006) 051606.

[3] EU-Directive 2002/95/EC: Restriction of the use of certain hazardous substances in electrical and electronic equipment (RoHS), Off. J. Eur. Union. 46 (2003) 19.

[4] Y. Saito, H. Takao, T. Tani, T. Nonoyama, K. Takatori, T. Homma, T. Nagaya, M. Nakamura, Lead-free piezoceramics, Nature. 432 (2004) 84.

[5] C. Kang, J.-H. Park, D. Shen, H. Ahn, M. Park, D.-J. Kim, Growth and characterization of $(K_{0.5}Na_{0.5})NbO_3$ thin films by a sol–gel method, J. Sol-Gel Sci. Technol. 58 (2010) 85–90.

[6] J.S. Kim, S.Y. Lee, C.W. Ahn, H.I. Hwang, H.J. Lee, S.H. Bae, I. W. Kim, Leakage Current Characteristics of Lead-Free $K_{0.5}Na_{0.5}NbO_3$ Ferroelectric Thin Films with (K,Na) Excess and Li Substitution, Jpn. J. Appl. Phys. 49 (2010) 095805.

[7] K. Tanaka, K. Kakimoto, H. Ohsato, T. Iijima, Effects of Pt Bottom Electrode Layers and Thermal Process on Crystallinity of Alkoxy-Derived $(Na,K)NbO_3$ Thin Films, Jpn. J. Appl. Phys. 46 (2007) 1094–1099.

[8] C.W. Ahn, S.Y. Lee, H.J. Lee, a Ullah, J.S. Bae, E.D. Jeong, J. S. Choi, B. H. Park, I. W. Kim, The effect of K and Na excess on the ferroelectric and piezoelectric properties of $K_{0.5}Na_{0.5}NbO_3$ thin films, J. Phys. D. Appl. Phys. 42 (2009) 215304.

[9] T. Saito, T. Wada, H. Adachi, I. Kanno, Pulsed Laser Deposition of High-Quality $(K,Na)NbO_3$ Thin Films on $SrTiO_3$ Substrate Using High-Density Ceramic Targets, Jpn. J. Appl. Phys. 43 (2004) 6627–6631.

[10] K. Shibata, F. Oka, A. Nomoto, T. Mishima, I. Kanno, Crystalline Structure of Highly Piezoelectric (K,Na)NbO_3 Films Deposited by RF Magnetron Sputtering, Jpn. J. Appl. Phys. 47 (2008) 8909–8913.

[11] K. Suenaga, K. Shibata, K. Watanabe, A. Nomoto, F. Horikiri, T. Mishima, Effect of Lattice Strain and Improvement of the Piezoelectric Properties of (K,Na)NbO_3 Lead-Free Film, Jpn. J. Appl. Phys. 49 (2010) 09MA05.

[12] T. Otsuki, K. Arita, Quantum jumps in FeRAM technology and performance, Integr. Ferroelectr. 17 (1997) 31–43.

[13] Q. Yu, J.-F. Li, Y. Chen, L.-Q. Cheng, W. Sun, Z. Zhou, Z. Wang, Effect of Pyrolysis Temperature on Sol-Gel Synthesis of Lead-free Piezoelectric (K,Na)NbO_3 Films on Nb:$SrTiO_3$ Substrates, J. Am. Ceram. Soc. 97 (2014) 107–113.

[14] D. Gao, K.W. Kwok, D. Lin, H.L.W. Chan, Microstructure and electrical properties of La-modified $K_{0.5}Na_{0.5}NbO_3$ lead-free piezoelectric ceramics, J. Phys. D. Appl. Phys. 42 (2009) 035411.

[15] A. Chowdhury, J. Bould, M.G.S. Londesborough, E. Večerníková, S.J. Milne, Evidence of phase heterogeneity in sol–gel $Na_{0.5}K_{0.5}NbO_3$ system, Mater. Chem. Phys. 124 (2010) 159–162.

[16] A. Chowdhury, J. Bould, M.G.S. Londesborough, S.J. Milne, The effect of refluxing on the alkoxide-based sodium potassium niobate sol–gel system: Thermal and spectroscopic studies, J. Solid State Chem. 184 (2011) 317–324.

[17] K. Tanaka, H. Hayashi, K. Kakimoto, H. Ohsato, T. Iijima, Effect of (Na,K)-Excess Precursor Solutions on Alkoxy-Derived (Na,K)NbO_3 Powders and Thin Films, Jpn. J. Appl. Phys. 46 (2007) 6964–6970.

[18] Y. Nakashima, W. Sakamoto, T. Shimura, T. Yogo, H. Maiwa, Lead-Free Piezoelectric (K,Na)NbO_3 Thin Films Derived from Metal Alkoxide Precursors, Jpn. J. Appl. Phys. 46 (2007) 6971–6975.

[19] K. Wang, J.-F. Li, Analysis of crystallographic evolution in (Na,K)NbO_3-based lead-free piezoceramics by x-ray diffraction, Appl. Phys. Lett. 91 (2007) 262902.

[20] K. Tanaka, K. Kakimoto, H. Ohsato, Fabrication of highly oriented lead-free (Na, K)NbO_3 thin films at low temperature by Sol–Gel process, J. Cryst. Growth. 294 (2006) 209–213.

[21] W. Gong, J.-F. Li, X. Chu, L. Li, Effect of pyrolysis temperature on preferential orientation and electrical properties of sol-gel derived lead zirconate titanate films, J. Eur. Ceram. Soc. 24 (2004) 2977–2982.

[22] A. Kupec, B. Malic, J. Tellier, E. Tchernychova, S. Glinsek, M. Kosec, Lead-Free Ferroelectric Potassium Sodium Niobate Thin Films from Solution: Composition and Structure, J. Am. Ceram. Soc. 95 (2012) 515–523.

[23] Q. Yu, J.-F. Li, W. Sun, Z. Zhou, Y. Xu, Z.-K. Xie, F-P. Lai, Q.-M.Wang, Electrical properties of $K_{0.5}Na_{0.5}NbO_3$ thin films grown on Nb:$SrTiO_3$ single-crystalline substrates with different crystallographic orientations, J. Appl. Phys. 113 (2013) 024101.

[24] K. Kakimoto, K. Akao, Y. Guo, H. Ohsato, Raman Scattering Study of Piezoelectric $(Na_{0.5}K_{0.5})NbO_3$ -$LiNbO_3$ Ceramics, Jpn. J. Appl. Phys. 44 (2005) 7064–7067.

[25] C.W. Ahn, H.-I. Hwang, K.S. Lee, B.M. Jin, S. Park, G. Park, D. Yoon, H. Cheong, H.-J. Lee, I. W. Kim, Raman Spectra Study of $K_{0.5}Na_{0.5}NbO_3$ Ferroelectric Thin Films, Jpn. J. Appl. Phys. 49 (2010) 095801.

[26] L. Wang, W. Ren, K. Yao, P.C. Goh, P. Shi, X. Wu, X. Yao, Effect of Pyrolysis Temperature on $K_{0.5}Na_{0.5}NbO_3$ Thick Films Derived from Polyvinylpyrrolidone-Modified Chemical Solution, J. Am. Ceram. Soc. 93 (2010) 3686–3690.

[27] P.C. Goh, K. Yao, Z. Chen, Lead-free piezoelectric $(K_{0.5}Na_{0.5})NbO_3$ thin films derived from chemical solution modified with stabilizing agents, Appl. Phys. Lett. 97 (2010) 102901.

[28] X. Yan, W. Ren, X. Wu, P. Shi, X. Yao, Lead-free (K, Na)NbO_3 ferroelectric thin films: Preparation, structure and electrical properties, J. Alloys Compd. 508 (2010) 129–132.

[29] R. Zuo, M. Wang, B. Ma, J. Fu, T. Li, Sintering and electrical properties of $Na_{0.5}K_{0.5}NbO_3$ ceramics modified with lanthanum and iron oxides, J. Phys. Chem. Solids. 70 (2009) 750–754.

[30] Y.-J. Dai, X.-W. Zhang, K.-P. Chen, Morphotropic phase boundary and electrical properties of $K_{1-x}Na_xNbO_3$ lead-free ceramics, Appl. Phys. Lett. 94 (2009) 042905.

[31] R. Zuo, J. Rodel, R. Chen, L. Li, Sintering and Electrical Properties of Lead-Free $Na_{0.5}K_{0.5}NbO_3$ Piezoelectric Ceramics, J. Am. Ceram. Soc. 89 (2006) 2010–2015.